

A Seven-membered Heterocycle Containing Coumarin Derivative with Aggregation Induced Emission Property

Deikrisha Lyngdoh Lyngkhoi^a and Snehadrinarayana Khatua^{a*}

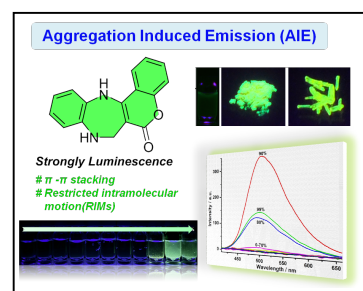
^aCentre for Advanced Studies, Department of Chemistry, North Eastern Hill University, Shillong, Meghalaya 793022, India.

Email: snehadri@gmail.com; skhatua@nehu.ac.in

Received: December 12, 2024 | Accepted: February 27, 2025 | Published online: March 18, 2025

Abstract

The development of seven-membered ring derivatives containing a coumarin moiety is crucial for biological applications, though it remains a challenging task. In this study, we designed and successfully synthesized two novel coumarin-based compounds, **Cou-EDA** and **Cou-OPD**, which incorporate a seven-membered ring modified with ethylenediamine and *o*-phenylenediamine, respectively. The structures of these compounds were fully characterized using 1D NMR (¹H and ¹³C) and ESI-HRMS spectrometry. **Cou-EDA** exhibits weak luminescence in both solution and solid states. However, the introduction of *o*-phenylenediamine in **Cou-OPD**, which adds an additional ring attached to the seven-membered structure, significantly enhances luminescence in both aggregated and solid states, producing a bright green emission. **Cou-OPD** demonstrates aggregation-induced emission (AIE) enhancement in poor solvents due to the formation of nanoaggregates and the restriction of intramolecular motion (RIM). To confirm the formation of nanoaggregates and to explore the morphology of the aggregate particles, dynamic light scattering (DLS) and scanning electron microscopy (SEM) analyses were conducted.



Keywords: Coumarin, Seven membered heterocycle, Aggregation Induced Emission

1. Introduction

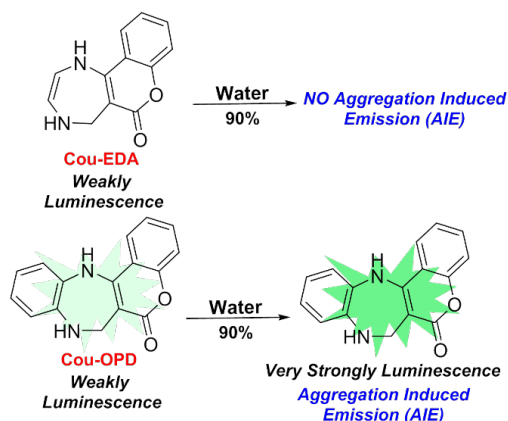
Development of small organic compound-based aggregation induced emission (AIE) luminogens has attracted greater attention in recent years and has a promising application in several research fields such as organic light emitting diode (OLED),^{1,2,3} sensing,^{4,5,6} and bioimaging.^{7,8,9} However, most organic luminogens that exhibit strong fluorescence in solution become weakly emissive or non-emissive upon aggregation or in the solid state, a phenomenon known as aggregation-caused quenching (ACQ). This leads to weak or quenched fluorescence at higher concentrations or in solid-state materials, limiting the practical application of these luminogens. To address the ACQ effect, Tang et al. introduced a new phenomenon in 2002 called Aggregation-Induced Emission (AIE), which is the inverse of the ACQ effect.^{10,11} AIE-active luminogens (AIEgens) are typically non- or weakly emissive in solution but exhibit strong fluorescence when in the form of nanoaggregates or in the solid state.^{12,13} The key factor driving the AIE effect is the restriction of intramolecular motion (RIM) caused by supramolecular interaction such as halogen bonding, hydrogen bonding,

$\pi \cdots \pi$ stacking, and C-H $\cdots\pi$ interaction.^{14,15,16} Apart from RIM, several processes such as *J*-aggregate formation, planarization, *E-Z* isomerization, twisted intramolecular charge transfer (TICT), and excited state intramolecular charge transfer (ESIPT), contribute to the AIE phenomenon.^{17,18,19,20} As a result, the development of organic AIE-active luminophores is of great importance and holds considerable potential for advancing a wide range of applications.²¹

To date, several AIE molecules have been developed, but rarely an AIE-active seven-membered coumarin derivative has been reported.²² Coumarin, a well-known chromophore and a naturally occurring organic compound abundant in many plants, plays a significant role in various biological activities, including anticancer, antioxidant, anticoagulant, antiviral, and antibacterial effects.^{23,24} It has a wide range of applications in several fields, such as detecting toxic ions, environmental protection, pharmacological activity, and fluorescence dye.^{25,26,27,28} Additionally, they are frequently used as chemosensors for detecting various analytes due to their unique photophysical properties, high quantum yield, excellent biocompatibility, and cell membrane permeability, as well as their ease of

synthesis and modification.^{29,30,31,32} Coumarin derivatives often shows a high fluorescence efficiency in solution state, but their planar coumarin skeleton are prone to form strong π - π stacking interactions in the aggregated or solid states.^{33,34,35,36} Despite this, several coumarin-based molecules have been developed as effective fluorescent probes for sensing toxic analytes.^{37,38,39,40,41,42} So far, the coupling of a seven-membered ring with coumarin to create AIE-active compounds remains underexplored. The seven-membered ring is a crucial structural motif found in many natural products and biologically active molecules, making its incorporation into coumarin derivatives particularly interesting.

In this context, we successfully synthesized a seven-membered coumarin-based compound using ethylene diamine (EDA) and o-phenylenediamine (OPD) as mediators, resulting in **Cou-EDA** and **Cou-OPD**, respectively (Scheme 1). Upon reduction, the free NH_2 group of o-phenylenediamine and ethylene diamine undergoes cyclization, eliminating the Cl-group on the coumarin moiety and forming a stable 7-membered heterocyclic compound. **Cou-EDA** emits very weakly in dilute solution but brightly in aggregated form or in solid state, whereas **Cou-OPD** in diluted solvent shows very weak luminescence but upon aggregation and in a solid state emit very strongly with highly green luminescence which is the indication of aggregation induced emission (AIE) property. The AIE property of **Cou-OPD** was further studied, the PL intensity is enhanced in the binary solvent mixtures, MeOH:H₂O and THF:H₂O at 90% water fraction, respectively. The DLS and SEM study was performed to further support the nano-aggregated formation of **Cou-OPD** in both solvent mixtures. To the best of our



Scheme 1: Schematic representation of **Cou-EDA** and **Cou-OPD** showing AIE.

knowledge, this is the first reported seven-membered heterocycle containing coumarin derivative with AIE-active property.

2. Experimental Section

2.1. Material and physical measurement.

All chemicals employed for the synthesis and sensing application were used as received without further purification from commercial suppliers such as Sigma-Aldrich, Alfa Aesar, and Spectrochem India. Infrared spectra were recorded using a PerkinElmer FT-IR Spectrometer in the range of 4000-400 cm^{-1} with KBr pellets. All 1D NMR (^1H and ^{13}C) spectra were recorded on a Bruker AVANCE II (400 MHz) spectrometer, taking chemical shift value in parts per million (ppm) and using residual protic solvent as the internal standard. High-resolution mass spectroscopy data was collected on Waters Xevo G2-XS QToF mass spectrometer connected to the ACQUITY UPLC I-Class System via an electrospray ionization (ESI) interface. All the NMR and ESI-HRMS spectra were processed in MestReNova software (version V12.0.0-20080). The UV-vis spectra were recorded in Agilent Cary 60 UV-vis spectrophotometer and PL spectra in PerkinElmer LS-55 and Agilent Cary Eclipse Fluorescence spectrophotometer with a quartz cuvette (path length = 1 cm), respectively. All spectroscopic measurement were performed in distilled acetonitrile solvent. The excitation and emission slit were set at 5 mm with the PMT voltage fixed at 700V.

2.2. Methodology for UV-vis experiments

In the UV-vis spectroscopic channel, the experiment was conducted as follows. The stock solution of the probe **Cou-EDA** and **Cou-OPD** was firstly prepared in 1 mM, which was later diluted to 0.01 mM using distilled acetonitrile. Before the measurement, the probe from the stock solution was diluted to 50 μM , and the spectra were recorded at room temperature, respectively. All the experiment were performed in distilled solvent and the samples for absorption measurement were contained in 1 cm \times 1 cm quartz cuvettes (3.5 ml volume).

2.3. Methodology for emission experiments

A stock solution (1 mM) of probe **Cou-EDA** and **Cou-OPD** was prepared 10-15 min earlier before the experiment in acetonitrile solution which was diluted to 0.01 mM. All spectroscopic measurement were maintained and performed in distilled solvent, and samples for emission measurement were contained in 1 cm \times 1 cm quartz cuvettes (3.5 mL

volume). The probe was excited at 300 nm for **Cou-EDA** and 350 nm for **Cou-OPD** and the excitation and the emission slit were set to 5 nm/5 nm, and the PMT voltage at 700 V.

2.4. Synthesis of 4-chloro-2-oxo-2H-chromen-3-carbaldehyde (Cou):

Following the reported procedure,³¹ the 4-Hydroxy-coumarin (1g, 0.005 mol) was dissolved in 6 mL anhydrous DMF and 2 mL of POCl₃ was added to the reaction mixture dropwise under continuous stirring at 0 °C. The mixture was allowed to reflux at 60 °C, for 1 hr and then cooled down at room temperature. Upon cooling the reaction mixture was slowly poured into crushed ice in an ice bath with continuous stirring and a yellow precipitate was obtained. The precipitate was kept in a refrigerator overnight, filtered and washed with water and dried under a vacuum. The product was recrystallised from acetone and isolated as yellow-colored crystals. Yield: 84% (0.935g). FTIR in KBr disk (ν/cm⁻¹): 3435, 3000, 1611, 1575, 1491, 1331, 1219, 761; (Figure 1) ¹H-NMR (400 MHz, CDCl₃): δ(ppm) = 10.38 (s, 1H), 8.12 (d, J = 7.2 Hz, 1H), 7.75 (d, J = 7.2 Hz, 1H), 7.49-7.40 (m, 2H). ¹³C NMR (100 MHz, CDCl₃): δ (ppm) 186.9, 158.4, 153.7, 153.3, 135.8, 127.7, 125.6, 118.4, 118.2, 117.1.

2.5. Synthesis of 2,3,4,5-tetrahydrochromeno[4,3-e][1,4]diazepin-6(1H)-one (Cou-EDA).

4-Chloro-3-formyl coumarin (0.208 g, 1 mmol) was dissolved in 20 mL of ethanol and added dropwise to 0.6mL EDA (ethylenediamine) under stirring condition over 30 minutes. An immediate colour change was observed from colourless to greenish. After 12 hours, the reaction was stopped and the formation of the corresponding Schiff base was confirmed by TLC. Dry NaBH₄ was added in small portion till the colour faded to whitish to reduce the Schiff base. After 1 hour of stirring the ethanol was evaporated under reduced pressure and the organic part was extracted using DCM. The DCM was evaporated under rotary evaporator and a whitish solid product was obtained. It was filtered, washed with ether, and dried in vacuo. Yield 61% (0.156 g). FTIR in KBr disk (ν/cm⁻¹): 3414, 2877, 1648, 1610, 1542, 1452, 1305, 1214, 889, 755. MS (ESI-HRMS; positive mode): (m/z, %): m/z = 217.0966 [(C₁₆H₁₂N₂O₂)⁺, 100%]; calcd. m/z = 217.0977; ¹H NMR (400 MHz, DMSO-d₆): δ (ppm) = 7.95 (d, J = 7.6 Hz, 1H), 7.53 (t, J = 8 Hz, 1H), 7.44 (s, 1H), 7.31-7.26 (m, 2H), 3.82 (s, 2H), 3.55 (q, J = 4.8 Hz, 2H), 3.00 (t, J = 5.6 Hz, 2H). ¹³C-NMR (100 MHz, DMSO-d₆): δ (ppm) = 162.0, 153.6,

151.6, 131.2, 123.4, 122.3, 116.6, 115.8, 98.1, 49.2, 45.6, 43.6.

2.6. Synthesis of 8,13-dihydrobenzo[b]chromeno[4,3-e][1,4]diazepin-6(7H)-one (Cou-OPD).

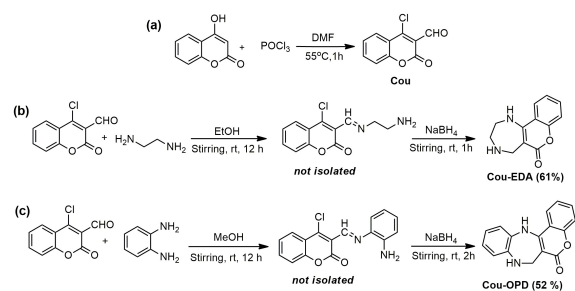
The **Cou-OPD** was synthesized following the similar procedure adopted for **Cou-EDA**. 4-Chloro-3-formyl coumarin, **Cou** (0.279 g, 1 mmol) was dissolved in 20 ml methanol and the dilution solution of **Cou** was added dropwise under stirring to the o-phenylenediamine (1.07 g, 10 mmol) solution (5 mL) over 30 minutes. An orange colour ppt was obtained immediately. After 12 hours, the reaction was stopped and the corresponding Schiff base was confirmed by TLC. Dry NaBH₄ was added portion wise to the mixture till colour faded to whitish to form the reduced Schiff base. Afterward, the reaction mixture was allowed to stir for 2 hours in room temperature, followed by the addition of 50 mL water and a yellow-colored ppt was obtained. It was filtered, washed with water and ether, and dry in vacuo. The ppt was recrystallized with acetone:methanol (3:1) to isolate a pure product. Yield 52 % (0.155 g). FTIR in KBr disk (ν/cm⁻¹): 3356, 3255, 1657, 1607, 1543, 1426, 1325, 1217, 898, 750, 611. MS (ESI-HRMS; positive mode): (m/z, %): 265.0972 [(C₁₆H₁₂N₂O₂)⁺, 100%]; calcd. m/z, 265.0975; ¹H NMR, (400 MHz, DMSO-d₆): δ 7.62 (d, J = 8.4 Hz, 1H), 7.55 (t, J = 8.0 Hz, 1H), 7.38 - 7.32 (m, 2H), 7.05 - 6.90 (m, 3H), 6.84 (d, J = 5.6 Hz, 1H), 4.39 (s, 2H), 2.17 (s, 1H). ¹³C NMR (100 MHz, DMSO-d₆): δ (ppm) = 162.5, 152.8, 145.9, 141.3, 131.9, 130.0, 124.5, 124.3, 122.1, 121.3, 120.8, 119.7, 118.5, 115.4, 99.9, 47.1.

3. Result and discussion

3.1 Synthesis and characterization

The compound **Cou** (4-chloro-2-oxo-2H-chromene-3-carbaldehyde) was synthesized following the reported procedure which was further used for the synthesis of **Cou-EDA** and **Cou-OPD**, using 4-hydroxycoumarin with POCl₃ in DMF as a solvent and isolated in good yield (84%). **Cou-EDA** and **Cou-OPD** were obtained by stirring ethanolic/methanolic solution of **Cou** with a dropwise addition of a saturated solution of o-phenylenediamine or ethylenediamine and allowed to stir for 12 hr followed by reduction by sodium borohydride at room temperature afforded a whitish and yellow-coloured product with 61% and 52% of yield respectively (Scheme 2). **Cou-EDA** and **Cou-OPD** were fully characterized by one-dimensional (1D) ¹H and ¹³C NMR

spectroscopy, and electron spray ionization mass spectroscopy (ESI-HRMS). The photophysical properties of both **Cou-EDA** and **Cou-OPD** were determined by UV-vis and photoluminescence (PL) spectroscopic methods. The NMR spectra of **Cou-EDA** and **Cou-OPD** were recorded in DMSO-d₆ at room temperature and clearly showed all expected peaks (Figure 2 and Figure 3). The ESI-HRMS spectra of **Cou-EDA** exhibit peaks at $m/z = 217.0977$ (calcd, $m/z = 217.0977$) and **Cou-OPD** exhibit peaks at $m/z = 265.0975$ (calcd, $m/z = 265.0972$) which is assigned to a single positive charged species (Figure 4).



Scheme 2: Synthetic procedure of (a) **Cou**, (b) **Cou-EDA** and (c) **Cou-OPD**.

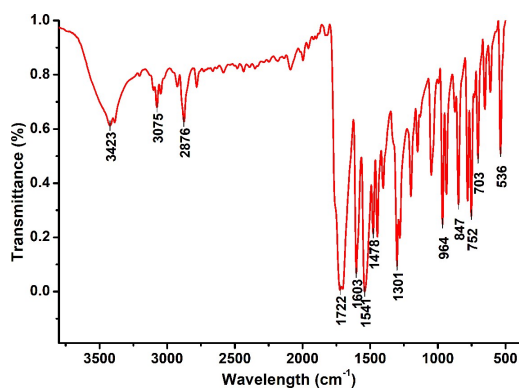


Figure 1: FT-IR spectrum of **Cou**

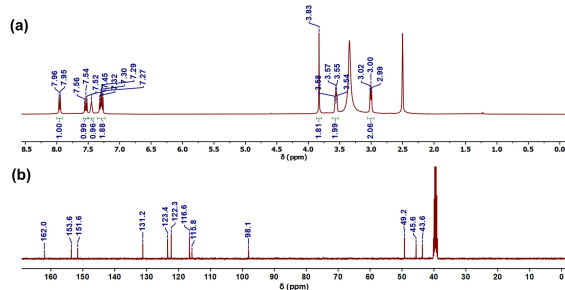


Figure 2: (a) ¹H and (b) ¹³C NMR spectra of **Cou-EDA** in DMSO-d₆.

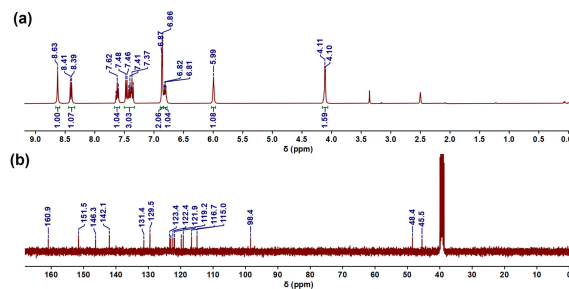


Figure 3: (a) ¹H and (b) ¹³C NMR spectra of **Cou-OPD** in DMSO-d₆

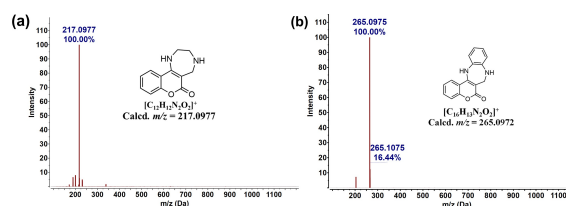


Figure 4: ESI-HRMS spectra of (a) **Cou-EDA** and (b) **Cou-OPD** in CH₃CN.

Aggregation Induced Emission Property

Cou-EDA (50 μM) displays the UV-vis spectral bands at ~ 318 nm ($\epsilon = 6486 \text{ M}^{-1} \text{ cm}^{-1}$), ~ 300 nm ($\epsilon = 5824 \text{ M}^{-1} \text{ cm}^{-1}$), ~ 231 nm ($\epsilon = 9943 \text{ M}^{-1} \text{ cm}^{-1}$) and ~ 215 nm ($\epsilon = 22781 \text{ M}^{-1} \text{ cm}^{-1}$) and the UV-vis spectrum of **Cou-OPD** (50 μM) shows bands at ~ 354 nm ($\epsilon = 3544 \text{ M}^{-1} \text{ cm}^{-1}$), ~ 307 nm ($\epsilon = 4968 \text{ M}^{-1} \text{ cm}^{-1}$), ~ 254 nm ($\epsilon = 1116 \text{ M}^{-1} \text{ cm}^{-1}$) and ~ 215 nm ($\epsilon = 17116 \text{ M}^{-1} \text{ cm}^{-1}$) in acetonitrile solution at 25°C respectively (Figure 5). These bands can be assigned to intraligand (IL) $\pi\text{-}\pi^*$ and $n\text{-}\pi^*$ transitions. Excitation of **Cou-EDA** at 300 nm results in a weakly green luminescence at 435 nm and excitation of **Cou-OPD** at 350 nm emits at 415 nm at room temperature (Figure 5a). **Cou-EDA** shows a weak luminescence in dilute solution, but in a solid powder or aggregated form does not show any luminescence (Figure 5b). However, **Cou-OPD** with a very weak luminescence in dilute solution shows bright green luminescence in the solid powder or crystalline form under the illumination of 365 nm UV lamp (Figure 5c). This observation leads to an indication of aggregation induced emission (AIE) behavior which is comparable to those of previously reported compounds that exhibit AIE. Firstly, the AIE property of **Cou-EDA** was examined in a binary solvent mixture. The PL spectra in MeOH and THF with increasing water fraction (0-99%) were recorded. In both the solvent mixtures, no such PL enhancement has been observed, which confirms the absence of aggregation induced emission (AIE) property

(Figure 6). Notably, the solid powder of **Cou-EDA** also did not show any luminescence and indicates the absence of AIE. The PL spectra **Cou-OPD** with increasing water fractions (0 to 99% of MeOH-H₂O and THF-H₂O) were recorded. In methanol, the PL intensity increases with increasing in water content (0-99%) and ~150 fold of PL enhancement is observed in the presence of 90% water and decreases at 99% of water (Figure 7a). The plot of PL intensity with increasing water fraction (0-99%) is shown in Figure 7b. The digital photograph under 365 nm UV illumination also shows an enhancement in green luminescence with increasing water fraction at 80% and 90%, which further decreases at 99% (Figure 7c). In THF, the PL intensity at 430 nm decreases gradually with increasing water content from 0-80% and shows a rapid enhancement at 500 nm with ~3 folds in the presence of 90% water which decreases at 99% of water in THF (Figure 8a). Similarly, the plot of water fraction (0-99%) vs PL intensity is shown in Figure 8b. The digital photograph shows an enhancement of green luminescence with increasing water fraction at 80-90% which drop at 99% (Figure 8c). These results indicate that **Cou-OPD** holds an AIE activity, which forms nano-aggregates at higher water fraction (f_w). The PL intensity in both MeOH:H₂O and THF:H₂O decrease at 99% of water, this decrease in the PL intensity is due to the formation of a crystalline aggregated or amorphous particles after the addition of water.

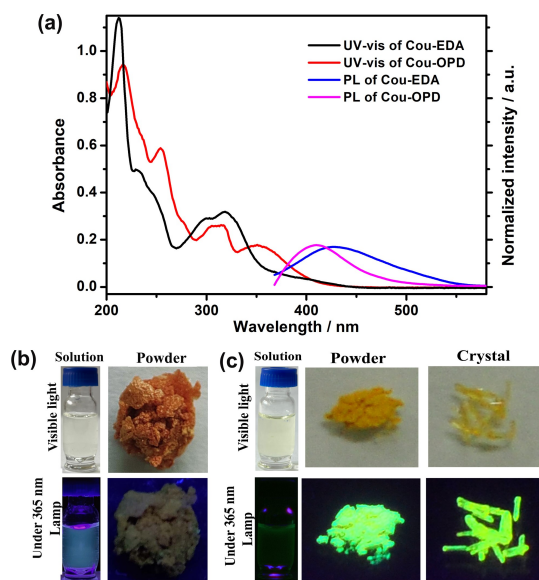


Figure 5. (a) Normalized UV-vis and PL spectra of **Cou-EDA** and **Cou-OPD**. Digital photos of (b) **Cou-EDA** (50 μ M) and (c) **Cou-OPD** (50 μ M) in CH₃CN solution and solid powder under an ambient light and UV light (365 nm) illumination.

Additionally, the UV-vis spectra of **Cou-OPD** (50 μ M, MeOH and THF) with increasing amount of water (0-99%) were recorded to support the aggregation. The absorption band and the UV-vis spectral line of **Cou-OPD** (50 μ M) were uplifted in both solvent mixtures with an increase in the water content, which ascribed to the light scattering by a nanoaggregate in solution (Figure 9a-9b). In a diluted solution, molecules exist in a non-aggregated states and an

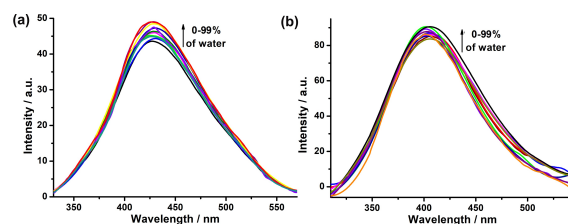


Figure 6. PL spectra of **Cou-EDA** (50 μ M, λ_{ex} = 300 nm) with increasing water fraction (0-99%) in (a) MeOH:H₂O and (b) THF:H₂O mixtures at room temperature.

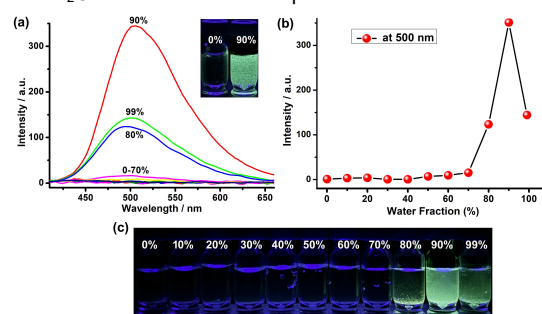


Figure 7. (a) PL spectra of **Cou-OPD** (50 μ M) with increasing water fraction (0-99%) in MeOH (λ_{ex} = 350 nm; λ_{em} = 500 nm) at room temperature (b) Plot of PL intensity vs water fraction. (c) Digital photograph of **Cou-OPD** in MeOH with different water fraction under 365 nm UV illumination.

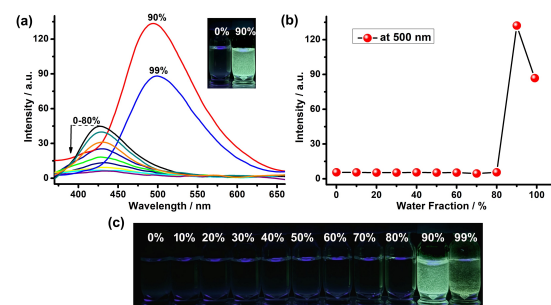


Figure 8. (a) PL spectra of **Cou-OPD** (50 μ M) with increasing water fraction (0-99%) in THF (λ_{ex} = 350 nm; λ_{em} = 500) solution at room temperature (b) Plot of emission intensity vs water fraction of water (c) Digital photograph of **Cou-OPD** in THF with different water fraction under 365 nm UV illumination.

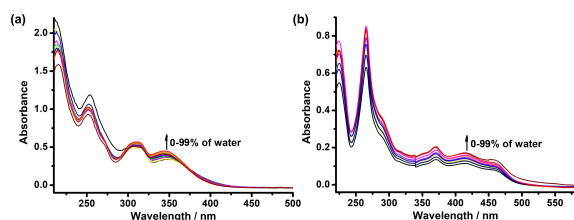


Figure 9. UV-vis spectra of **Cou-OPD** ($50 \mu\text{M}$, $\lambda_{\text{ex}} = 350 \text{ nm}$) with increasing water fraction (0-99%) (a) MeOH:H₂O and (b) THF:H₂O mixtures at room temperature.

intramolecular vibratory motion and upon excitation, release it energy through a non-radiative pathway through interacting solvent and consequently quench the luminescence. But in the aggregated state, the weak intermolecular interaction such as C-H $\cdots\pi$ stacking and hydrogen bonding interactions are present, which restrict the intramolecular motion and hence intensify the luminescence of **Cou-OPD**. The presence of an extra ring in **Cou-OPD** results in more conjugation and enhances in π - π stacking in the aggregated or solid states and hence shows aggregation induced emission (AIE) enhancement, whereas in **Cou-EDA**, the absence of the extra ring results in non-luminescence in the aggregated form or in the solid state.

Dynamic Light Scattering (DLS) and Scanning Electron Microscopy (SEM) Study

The aggregation property of **Cou-OPD** in MeOH:H₂O (1:9 v/v) and THF:H₂O (1:9 v/v) mixtures was further supported by dynamic light scattering (DLS) study. The hydrodynamic diameter of the aggregated particles at $f_w = 90\%$ ranges at 100 to 300 nm with the Z_{average} of 153.37 nm for MeOH:H₂O (1:9 v/v) and for THF:H₂O (1:9 v/v), ranges around 100 to 500 nm with the Z_{average} of 188.25 nm at $f_w = 90\%$ respectively (Figure 10a-10b). To visualize the morphology of the nano-aggregate particles, scanning electron microscope (SEM) images were taken under the same experimental condition at 90% of water in both solvent mixtures. The SEM image of **Cou-OPD** in MeOH:H₂O ($f_w = 90\%$) clearly shows the formation of a nano-aggregate with a spherical shape and a diameter ranging from ~ 100 to 500 nm (Figure 10c). Similarly, in THF:H₂O (1:9 v/v), nano-aggregated particles of **Cou-OPD** were observed ranges from ~ 100 nm to ~ 500 nm with the same spherical morphology in both the solvent mixture (Figure 10d). Thus the direct observation through SEM images clearly demonstrates the spherical nano-

aggregation of **Cou-OPD** in both MeOH:H₂O (1:9 v/v) and THF:H₂O (1:9 v/v) solvent mixtures.

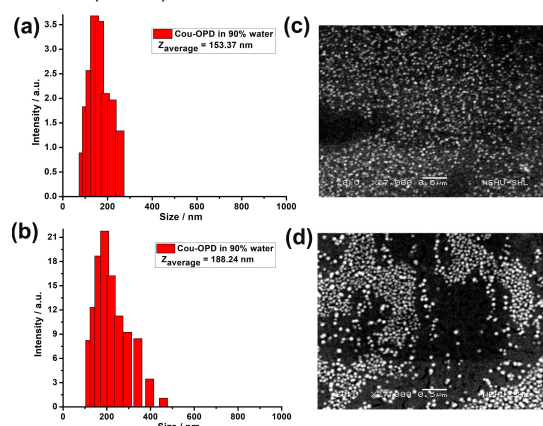


Figure 10. Particle size distribution of **Cou-OPD** ($50 \mu\text{M}$) in (a) MeOH:H₂O (b) THF:H₂O and SEM images of **Cou-OPD** in (c) MeOH:H₂O (d) THF:H₂O (1:9 v/v) solvent mixtures.

Conclusion

We have successfully developed two new seven-membered ring containing coumarin derivatives, **Cou-EDA** and **Cou-OPD** and fully characterized by ¹H, ¹³C spectroscopy and HRMS spectrometry. The probe, **Cou-EDA**, is weakly luminescent in solution state and non-luminescent in aggregated state and does not exhibit AIE property. The introduction of an extra ring in **Cou-OPD** enhanced the luminescence in the aggregated state and hence shows AIE property with a bright green luminescence in aggregated and solid state through restriction in intramolecular motion due to π - π stacking and intermolecular H-bonding. The AIE of **Cou-OPD** was studied in two different binary solvent mixtures with ~ 150 -fold and ~ 3 -fold PL intensity enhancement at 90% water fraction (f_w) in MeOH and in THF, respectively. The formation of the nano-aggregates of **Cou-OPD** was further confirmed by dynamic light scattering (DLS) and scanning electron microscopic studies. This AIE active seven-membered coumarin is very important and can be further applied in biological activity.

5. Acknowledgements

We thank SERB (CRG/2023/009059) for the financial assistance and Sophisticated Analytical and Instrumentation Facility (SAIF), North-Eastern Hill University, for NMR data. We also thank the DST-FIST program (No. SR/FST/CS-II/2019/ 99(C), Govt. of India for providing HRMS instrument to the Dept. of Chemistry, NEHU, Shillong. D.L.L thank North-Eastern Hill University for the research fellowship.

6. Notes and References

- Yang, J.; Fang, M.; Li, Z. Organic luminescent materials: The concentration on aggregates from aggregation-induced emission. *Aggregate* **2020**, *1*, 6–18.
- Yan, L.; Li, R.; Shen, W.; Qi, Z. Multiple-color AIE coumarin-based Schiff bases and potential application in yellow OLEDs. *Journal of Luminescence* **2018**, *194*, 151–155.
- Sun, Y.; Lei, Z.; Ma, H. Twisted aggregation-induced emission luminogens (AIEgens) contribute to mechanochromism materials: a review. *J. Mater. Chem. C* **2022**, *10*, 14834–14867.
- Wang, J.; Meng, Q.; Yang, Y.; Zhong, S.; Zhang, R.; Fang, Y.; Gao, Y.; Cui, X. Schiff Base Aggregation-Induced Emission Luminogens for Sensing Applications: A Review. *ACS Sens.* **2022**, *7*, 2521–2536.
- Chen, M.; Zhong, M.; Huang, S.; Chen, Y.; Cao, F.; Hu, H.; Huang, W.; Ji, D.; Zhu, M. α -Cyanostilbene-based sensor with "AIE and ESIPT" features emitting long-wavelength intense red-fluorescence for highly selective and sensitive detection of Cu^{2+} . *Inorganic Chemistry Communications* **2023**, *33*, 110640.
- Zalmi, G. A.; Gawade, V. K.; Nadimetta, D. N.; Bhosale, S. V. Aggregation Induced Emissive Luminogens for Sensing of Toxic Elements. *ChemistryOpen* **2021**, *10*, 681–696.
- Yan, L.; Zhang, Y.; Xu, B.; Tian, W. Fluorescent nanoparticles based on AIE fluorogens for bioimaging. *Nanoscale* **2016**, *8*, 2471–2487.
- Shellaiah, M.; Sun, K.-W. Pyrene-Based AIE Active Materials for Bioimaging and Theranostics Applications. *Biosensors* **2022**, *12*, 550.
- Mei, J.; Huang, Y.; Tian, He., Progress and Trends in AIE-Based Bioprobes: A Brief Overview. *ACS Appl. Mater. Interfaces* **2018**, *10*, 12217–12261.
- Luo, J.; Xie, Z.; Lam, J. W. Y.; Cheng, L.; Chen, H.; Qiu, C.; Kwok, H. S.; Zhan, X.; Liu, Y.; Zhu, D.; Tang, B. Z. Aggregation induced emission of 1-methyl-1,2,3,4,5-pentaphenylsilole. *Chem. Commun* **2001**, 1740–1741.
- Ma, S.; Du, S.; Pan, G.; Dai, S.; Xu, B.; Tian, W. Organic molecular aggregates: From aggregation structure to emission property. *Aggregate* **2021**, *2*, e96.
- Hong, Y.; Lam, J. W. Y.; Tang, B. Z. Aggregation-induced emission. *Chem. Soc. Rev* **2011**, *40*, 5361–5388.
- Zhao, Z.; Zhang, H.; Lam, J. W. Y.; Tang, B. Z. Aggregation-Induced Emission: New Vistas at the Aggregate Level. *Angew. Chem. Int. Ed* **2020**, *59*, 9888–9907
- Ji, C.; Lai, L.; Li, P.; Wu, Z.; Cheng, W.; Yin, Meizhen. Organic dye assemblies with aggregation-induced photophysical changes and their bio-applications. *Aggregate* **2021**, *2*, e39.
- Peng, Q.; Shuai, Z. Molecular mechanism of aggregation-induced emission. *Aggregate* **2021**, *2*, e91.
- Ding, D.; Li, K.; Liu, B.; Tang, B. Z. Bioprobes Based on AIE Fluorogens. *Acc. Chem. Res* **2013**, *46*, 2441–2453.
- Sheet, S. K.; Sen, B.; Aguan, K.; Khatua, S. A cationic organoiridium(III) complex-based AIEgen for selective light-up detection of rRNA and nucleolar staining. *Dalton Trans.* **2018**, *47*, 11477–11490.
- Mei, J.; Leung, N. L. C.; Kwok, R. T. K.; Lam, J. W. Y.; Tang, B. Z. Aggregation-Induced Emission: Together We Shine, United We Soar!. *Chem. Rev* **2015**, *115*, 11718–11940.
- Chen, W.; Zhang, C.; Han, X.; Hua, S. H.; Tan, Y.; Yin, J. Fluorophore-Labeling Tetraphenylethene Dyes Ranging from Visible to Near-Infrared Region: AIE Behavior, Performance in Solid State, and Bioimaging in Living Cells. *J. Org. Chem* **2019**, *84*, 14498–14507.
- Hu, Q.; Gong, T.; Mao, Y.; Yin, Q.; Wang, Y.; Wang, H. Two-phase activated colorimetric and ratiometric fluorescent sensor for visual detection of phosgene via AIE coupled TICT processes. *Spectrochimica Acta Part A: Molecular and Biomolecular Spectroscopy* **2021**, *253*, 119589.
- Patra, S. K.; Sen, B.; Rabha, M.; Khatua, S. An aggregation-induced emission-active bis-heteroleptic ruthenium(II) complex of thiophenyl substituted phenanthroline for the selective "turn-off" detection of picric acid. *New J. Chem* **2022**, *46*, 169.
- Bu, F.; Duan, R.; Xie, Y.; Yi, Y.; Peng, Q.; Hu, R.; Qin, A.; Zhao, Z.; Tang, B. Z. Unusual Aggregation-Induced Emission of a Coumarin Derivative as a Result of the Restriction of an Intramolecular Twisting Motion. *Angew Chem* **2015**, *127*, 14700–14705.
- Cao, D.; Liu, Z.; Verwilt, P.; Koo, S.; Jangjili, P.; Kim, J. S.; Lin, W. Coumarin-Based Small-Molecule Fluorescent Chemosensors. *Chem. Rev* **2019**, *119*, 10403–10519.
- Lee, J. H.; Kim, K. Y.; Jin, H.; Baek, Y. E.; Choi, Y.; Jung, S. H.; Lee, S. S.; Bae, J.; Jung, J. H. Self-Assembled Coumarin Nanoparticle in Aqueous Solution as Selective Mitochondrial-Targeting Drug Delivery System. *ACS Appl. Mater. Interfaces* **2018**, *10*, 3380–3391.
- Naik, V. G.; Hiremath, S. D.; Thakuri, A.; Hemmadi, V.; Biswas, M.; Banerjee, M.; Chatterjee, A. A coumarin coupled tetraphenylethylene based multi-targeted AIEgen for cyanide ion and nitro explosive detection, and cellular imaging. *Analyst* **2022**, *147*, 2997–3006.
- Huanga, Li.; Sheng, W.; Wang, L.; Meng, X.; Duan, H.; Chi, L. A novel coumarin-based colorimetric and fluorescent probe for detecting increasing concentrations of Hg^{2+} in vitro and in vivo. *RSC Adv* **2021**, *11*, 23597–23606.
- Meng, Q.; Bai, C.; Yao, J.; Wang, X.; He, S.; Liu, X.; Wang, S.; Xue, W.; Zhang, L.; Wei, B.; Miao, H.; Qu, C.; Qiao, R. Dual-mode "turn-on" fluorescence and colorimetric probe toward cyanide based on ESIPT and its bioimaging applications. *Journal of Luminescence* **2023**, *263*, 120031.
- Pooja.; Pandey, H.; Aggarwal, S.; Vats, M.; Rawat, V.; Pathak, S. R. Coumarin-based Chemosensors for Metal Ions Detection. *Asian Journal of Organic Chemistry* **2022**, *12*, e202200455.
- Sun, X.-y.; Liu, T.; Sun, J.; Wang, X.-j. Synthesis and application of coumarin fluorescence probes. *RSC Adv* **2020**, *10*, 10826–10847.

30. Kou, J.; Meng, Z.; Wang, X.; Wang, Z.; Yang, Y. A novel coumarin derivative-modified cellulose fluorescent probe for selective and sensitive detection of CN⁻ in food samples. *Anal. Methods* **2023**, *15*, 1639-1648.
31. Lyngkhai, D. L.; Khatua, S. A coumarin containing hemicyanine-based probe for dual channel detection of cyanide ion. *Inorganica Chimica Acta* **2024**, *572*, 122300.
32. Fan, Y.; Wu, Y.; Hou, J.; Wang, P.; Peng, X.; Ge, G. Coumarin-based near-infrared fluorogenic probes: Recent advances, challenges and future perspectives. *Coordination Chemistry Reviews* **2023**, *480*, 215020.
33. Singh, A.; Yadav, P.; Singh, S.; Kumar, P.; Srikrishna, S.; Singh, V. P. A multifunctional coumarin-based probe for distinguishable detection of Cu²⁺ and Zn²⁺: its piezochromic, visochromic and AIE behavior with real sample analysis and bio-imaging applications. *J. Mater. Chem. C* **2023**, *11*, 13056-13066.
34. Zhang, K.; Shu, J.; Chu, W.; Liu, X.; Xu, B.; Jiang, W. Rational design of coumarin fluorophore with solvatochromism, AIE and mechanofluorochromic enhancement properties. *Dyes and Pigments* **2021**, *185*, 108898.
35. Qian, R.; Tong, H.; Huang, C.; Li, J.; Tang, Y.; Wang, R.; Lou, K.; Wang, W. A donor–acceptor triptycene–coumarin hybrid dye featuring a charge separated excited state and AIE properties. *Org. Biomol. Chem* **2016**, *14*, 5007-5011.
36. Shamsiya, A.; Bahulayan, D. D–A systems based on oxazolone–coumarin triazoles as solid-state emitters and inhibitors of human cervical cancer cells (HeLa). *New J. Chem* **2022**, *46*, 480-489.
37. Xia, H. C.; Xu, X. H.; Song, Q. H. A fluorescent chemosensor for selective detection of phosgene in solutions and in gas phase. *ACS Sens* **2017**, *2*, 178–182.
38. Hu, Q.; Song, Y. F.; Wu, W. N.; Zhao, X.-L.; Wang, Y.; Fan, Y.-C. A coumarin-pyrazole-based probe for the fluorescence detection of phosgene with high selectivity and sensitivity. *Anal. Methods* **2023**, *15*, 2761.
39. Zhu, D.; Rajalakshmi, K.; Wang, R.; Wu, H.; Kanna, P.; Song, J. -W.; Lee, H. -J.; Muthusamy, S. A coumarin derivative-based turn-on fluorescent probe for real-time applications of hydrazine detection in environment and bioimaging. *Dyes and Pigments* **2023**, *216*, 111370.
40. Majhi, A.; Venkateswarlu, K.; Sasikumar, P. Coumarin Based Fluorescent Probe for Detecting Heavy Metal Ions. *Journal of Fluorescence* **2024**, *34*, 1453–1483.
41. Feng, W.; Gong, S.; Zhou, E.; Yin, X.; Feng, G. Readily prepared iminocoumarin for rapid, colorimetric and ratiometric fluorescent detection of phosgene. *Anal Chim Acta* **2018**, *1029*, 97–103.
42. Xie, Y.; Cheng, W.; Jin, B.; Liang, C.; Ding, Y.; Zhang, W. Solvent directed selective and sensitive fluorescence detection of target ions using a coumarin–pyridine probe. *Analyst* **2018**, *143*, 5583-5588

7. About the author(s)

Deikrisha Lyngdoh Lyngkhai is currently a PhD scholar at North-Eastern Hill University (NEHU), Shillong, Meghalaya working under the guidance of Dr. Snehadrinarayan Khatua. She completed her BSc at St. Mary's College Shillong, in 2017 and her MSc in Chemistry at NEHU, Shillong in 2019. She was admitted as a PhD scholar in 2021 and published 5 paper in international journal till date. She also received two best poster award at “Sustainability and Interdisciplinarity in Chemical Sciences



(SICS)-2023, IISER Kolkata, 2023” and “Recent Trends in Applied Sciences: A Special Focus on Nano-science & Nano-materials” (RTAS-2024) NEHU, Shillong, Meghalaya”. Her PhD research work includes development of small organic probes, Ru(II) and Ir(III) metal complexes and study their photoluminescent properties such as Aggregation Induced Emission, Solvatochromism and also applications of the strategically designed probes in sensing chemical warfare agents, toxic ions and bio imaging.

Dr. Snehadrinarayan Khatua is currently an Associate Professor at North-Eastern Hill University (NEHU), Shillong, Meghalaya. He received his PhD from IIT, Karagpur (2007),



under the guidance of Prof. Manish Battacharjee and worked as a Post-doctoral fellow at Korea Advanced Institute of Science and Technology (KAIST), South Korea (2007-2009) under Prof. David. G. Churchill. He was working as an Alexander von Humboldt(AvH) Fellow, Universität Siegen, Germany (2009-2011) under Prof. Michael Schmittel. He has over 62 international publication. In 2024, he received CRS Bronze Medal Award, Vidyasagar University, West Bengal. He is a fellow of the Indian Chemical Society (FICS), Calcutta, Chemical Research Society of India (CRSI), Bangalore and Chirantan Rasayan Sangstha (CRS), West Bengal. His research group works mainly on luminescent d⁶-metal such as Ru(II) and Ir(III) polypyridine complexes, organic dye molecules, and transition metal complex for diverse applications such as sensing, bioimaging, and photocatalysis.

Article Note: A collection of invited papers based on *Award Lecture* presentations in the International Symposium *Science Beyond Boundary: Invention, Discovery, Innovation and Society 'Rasayan 19'* held at IISER Kolkata during July 29-30, 2024.